

## 6.4 Ordered Phases

by Gerald Schlatte

Iron forms superlattice structures, i.e. ordered phases, with a large number of elements, some of which, e.g. silicon, aluminium, nickel, cobalt, vanadium and titanium, are used as alloy additions in various types of steels.

In superalloys ordered phases such as  $\text{Ni}_3\text{Al}$  lead to increased strength at high temperatures (see chapter 5 and 6.5). Such phases also occur in magnetic materials (see 6.6).

The nature of ordered phases and the contrast effects to be expected in the TEM are discussed briefly below. Since the number of possible ordered phases is very large, only a few examples from the field of substitution solid solutions will be presented. Detailed descriptions of the electron optical contrast effects in ordered alloys are given for example in <sup>6,7)</sup>.

### 6.4.1 The B2 and $\text{DO}_3$ structures as examples of ordered phases

Ordered phases occur frequently when attractive interactions exist between the elements present in an alloy. The atoms of one species A then try to surround themselves with nearest neighbours consisting only of the species B. Fig. 17 shows the situation for the body-centred cubic iron lattice. The atoms on the lattice I and II are nearest neighbours (n.n.) of the atoms on the sites III and IV. If the atoms are randomly distributed, the probability of finding an A-atom on a lattice site of a given sublattice L (L = I, II, III, IV) is equal to the concentration of A in the alloy. In the case of long-range order, there will be a deviation from this statistical distribution such that one or more sublattices are preferred by a particular atomic species.

In the body-centred cubic iron lattice, for example, the atoms of type A may occupy preferentially the sublattices I and II, and the atoms of type B the sublattices III and IV. This type of super-lattice is called the B2 structure. The A atoms are surrounded with B atoms as nearest neighbours. The stoichiometric ratio of the two species should be 1:1.

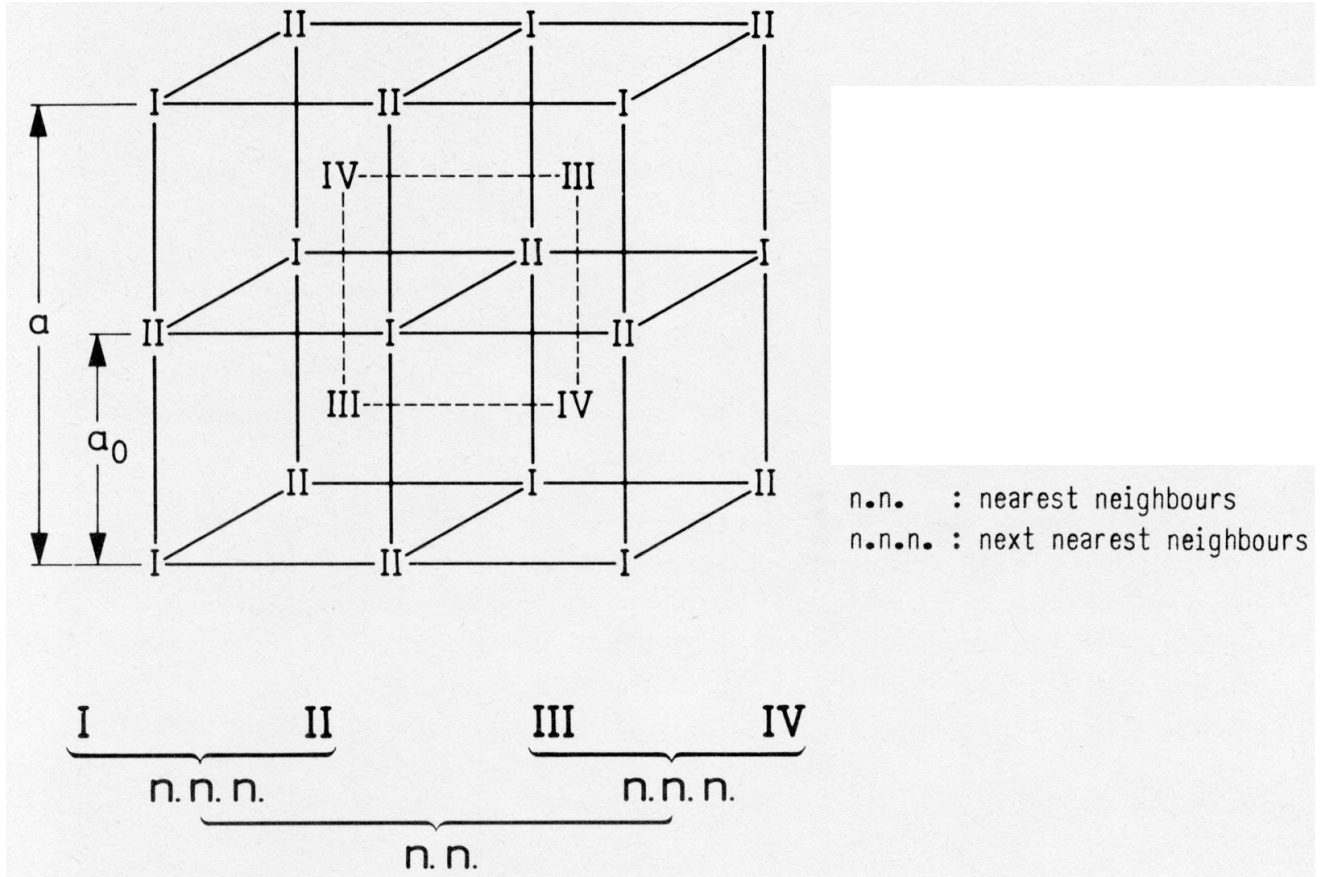


Fig. 17: Division of a body-centered cubic lattice into four face-centered cubic sublattices with the double lattice parameter



However, the range of existence of the B2 structure is very large, extending to 10 at. % Si in the case of the iron-silicon system.

If, in a crystal with body-centred cubic structure, the atoms B2 of type B are surrounded mainly with A atoms also as next nearest neighbours (n.n.n.) the DO<sub>3</sub> structure is formed. In Fig. 17 it may be seen that all the next nearest neighbours of atoms on the sublattice III lie on sites of the sublattice IV and vice versa. In this structure one species B would be found predominantly on the sublattice IV, and the other three sublattices would be occupied mainly by atoms of type A. The stoichiometric composition would be A<sub>3</sub>B, but the range of existence extends far beyond this. In the iron-silicon system, the DO<sub>3</sub> structure is found on slow cooling with silicon contents as low as about 13 at. %.

These two ordered phases will be treated as representatives of the superlattice phases, since they show the electron microscopical contrast effects characteristic for ordered phases in a typical fashion. It may be mentioned further that a body-centred cubic solid solution with random occupation of the lattice sites has the A2 structure.

## 6.4.2 Observation of ordered phases in the electron microscope

### 6.4.2.1 Electron diffraction of ordered crystals

With regard to their selected area electron diffraction patterns, ordered crystals may be distinguished from the disordered state by the occurrence of additional spots, since ordered crystals have additional periodicities in the lattice. As an example Fig. 18 shows a diffraction pattern of a DO<sub>3</sub> ordered iron-silicon crystal. The matrix spots arising from the basic body-centred cubic lattice and the additional spots due to ordering of nearest and next nearest neighbours (B2 and DO<sub>3</sub> spots) are indicated in the schematic diagram (Fig. 19).

Ordered phases which are completely free of lattice defects may thus be identified by their diffraction patterns. In addition, there are some lattice defects which occur only in ordered crystals. These are superlattice dislocation and antiphases boundaries (APB).

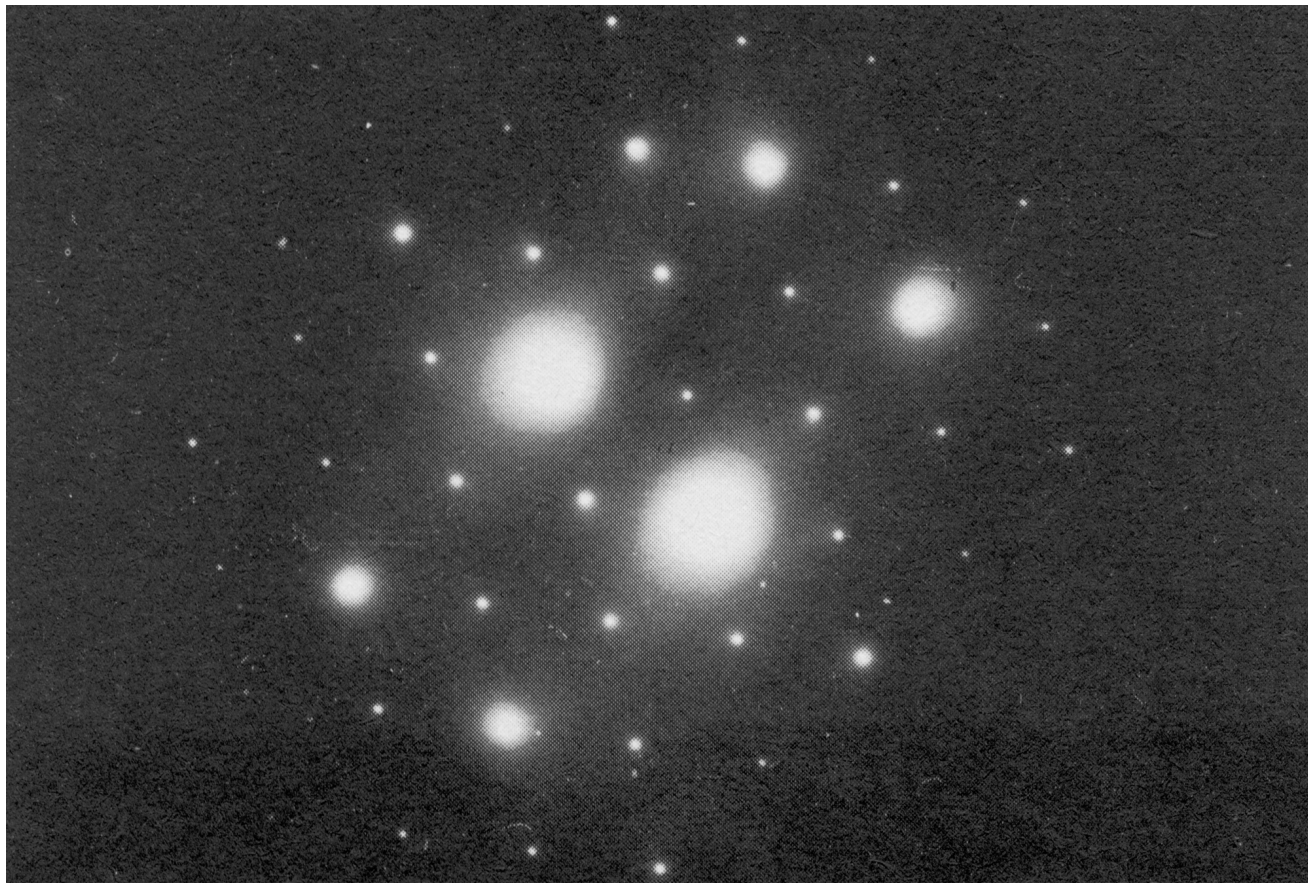


Fig. 18: Diffraction pattern of a  $\text{DO}_3$ -ordered iron-silicon crystal, zone axis  $[110]$

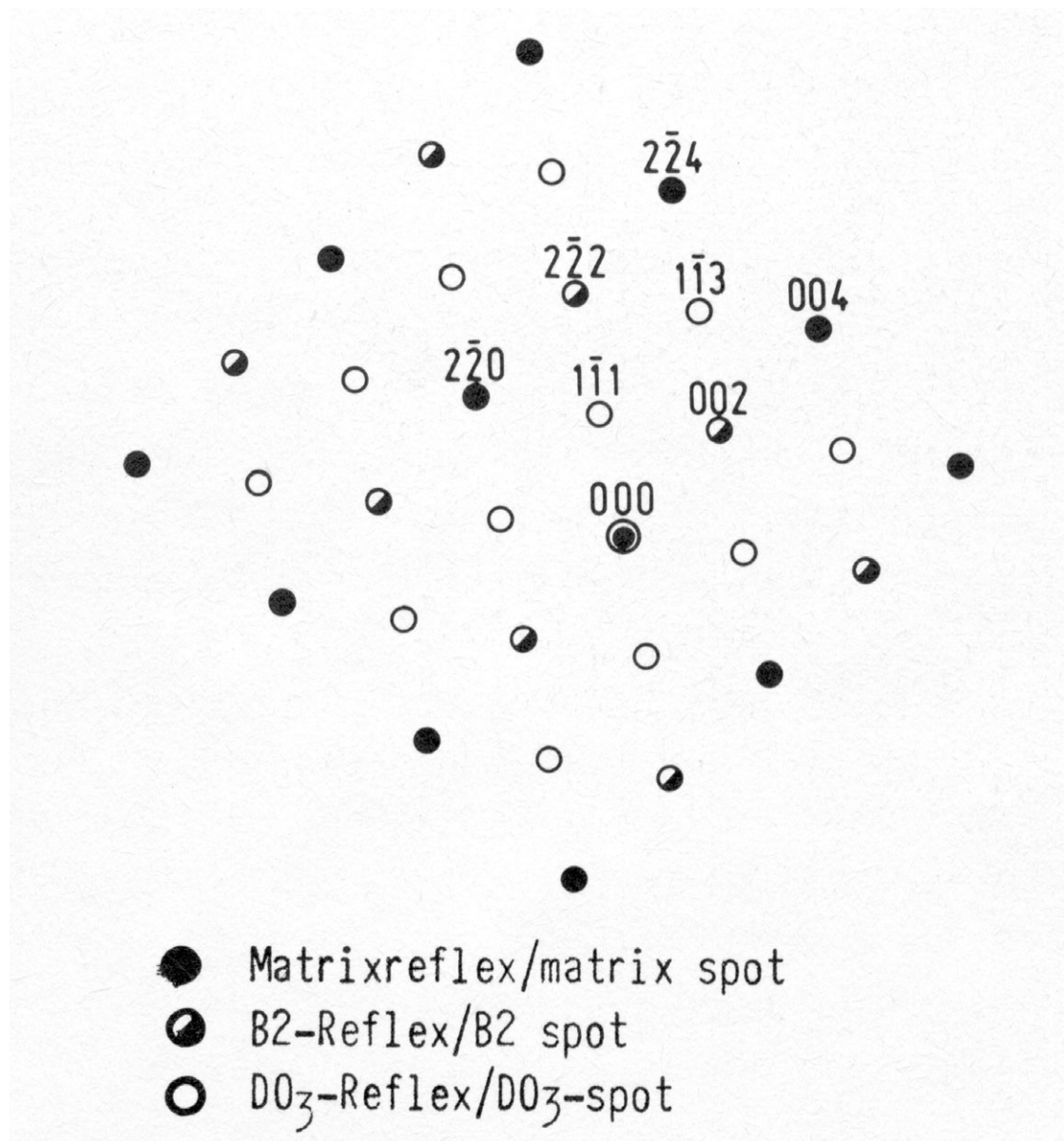


Fig. 19: Indexing of Fig. 18

### 6.4.2.2 Antiphase boundaries of thermal origin

Antiphase boundaries (APB) are two-dimensional lattice defects which do not affect the basic lattice of the crystal. The lattice positions are not changed. Along an APB there are neighbourhood relations between atoms which are not present in the undisturbed ordered crystal.

The formation of a thermal APB may be imagined as follows: above the critical ordering temperature, i.e. in the disordered state, there is no difference between the various sublattices. If the alloy is cooled, ordering takes place, starting from certain nucleation sites. In the case of the B2 structure, the sublattices I and II may be occupied preferentially by the A atoms at one nucleation site and by the B atoms at another site. Where these two crystal regions meet on growth an APB is formed with disturbed nearest neighbourhoods. In the case of the DO<sub>3</sub> structure, there is a second type of APB, at which only the next nearest neighbours are disturbed. Here the crystallographically equivalent but differently occupied sublattices III and IV exchange functions. An APB is characterised by the displacement vector  $r$  by which the two regions on each side of the APB must be displaced relative to one another to compensate the defect (Fig. 20).

The contrast at an APB imaged in the TEM can be explained in a similar way to stacking fault contrast. APBs are clearly visible in dark field if the condition  $g \cdot r \neq 0, 2\pi \dots$  is satisfied, where  $g$  is the reciprocal lattice vector of the diffracted beam used for imaging. This condition can be fulfilled only for superlattice spots, since an APB does not affect the basic lattice.

Superlattice spots are generally weaker than the matrix spots. Their extinction distance is therefore relatively large and often exceeds the foil thickness, APBs therefore do not show the periodical fringe contrast typical for stacking faults, but are visible as a dark band in the exact Bragg orientation (Fig. 21). The irregular form of the APBs indicates that they were formed during cooling of the crystal.

An important characteristic of APBs is the contrast reversal produced by tilting slightly away from the Bragg orientation at the edge of an extinction contour. With the aid of a



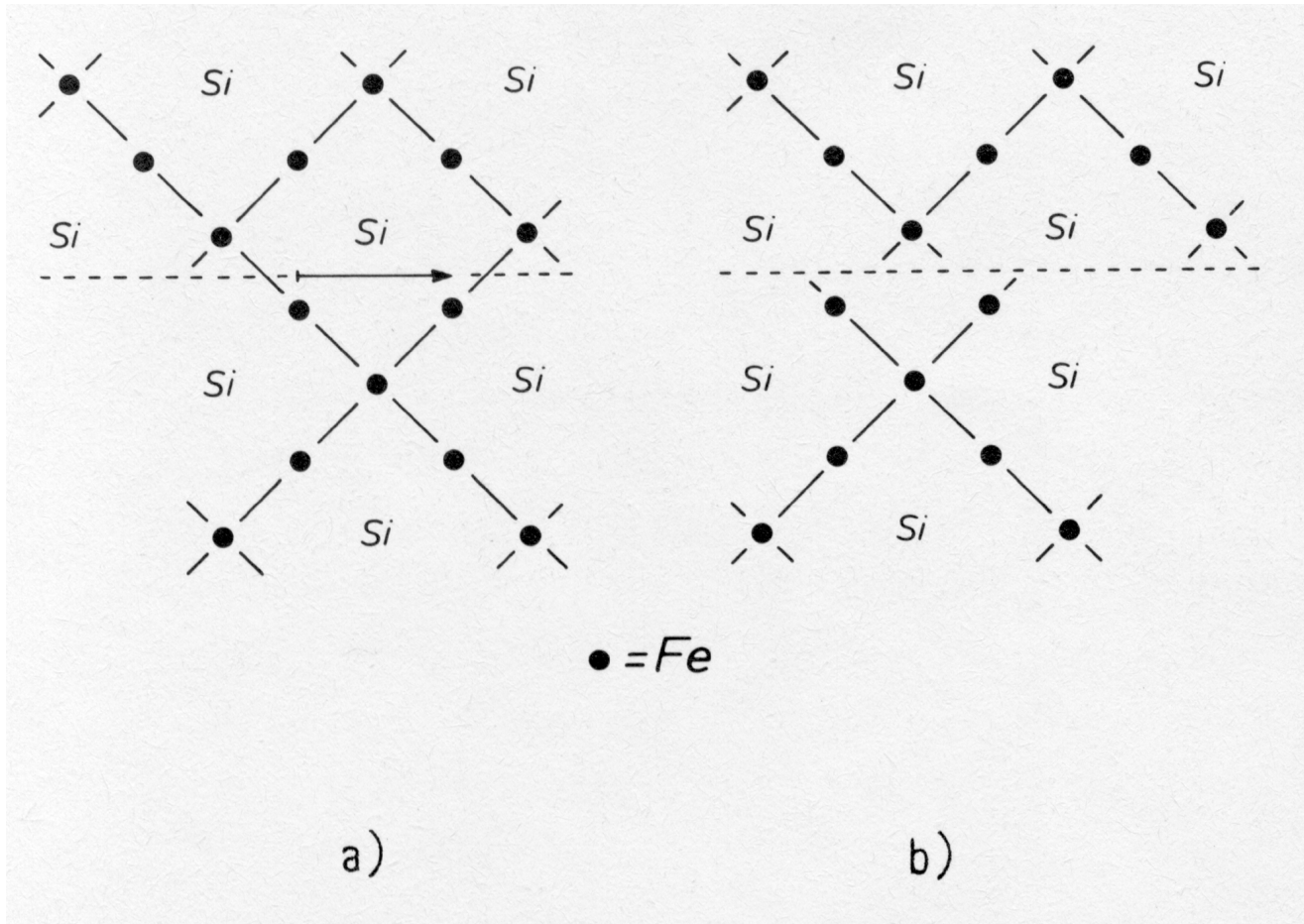


Fig. 20: Schematic diagram of an antiphase boundary in a two-dimensional crystal lattice

- a) perfect crystal with displacement vector
- b) antiphase boundary

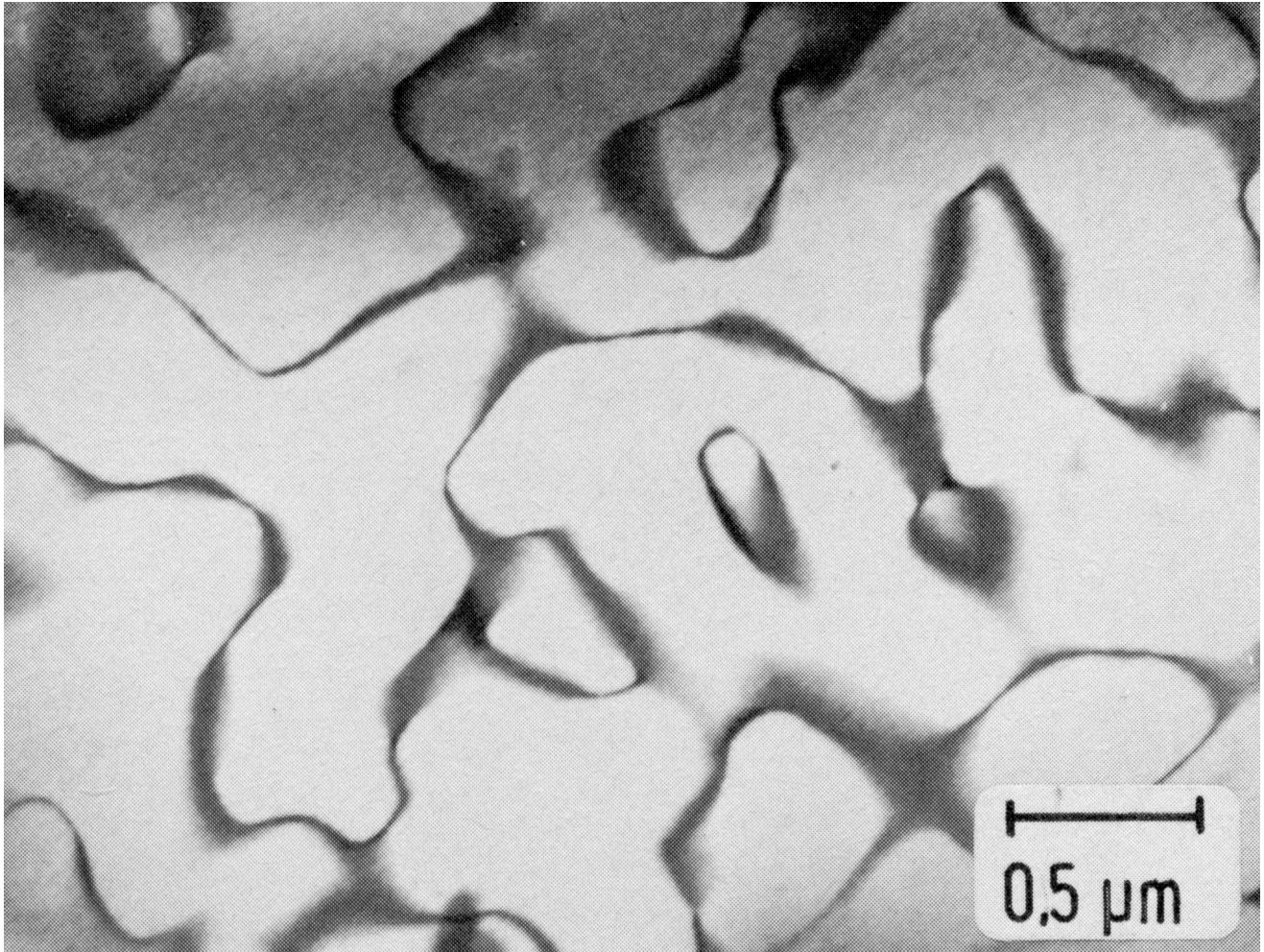


Fig. 21: Thermally formed antiphase boundary in a B2-ordered alloy (iron with 12 % Si): Dark field image with B2-superlattice spot, thin foil



goniometer stage this contrast reversal may be achieved in any area of the specimen (Fig. 22 and Fig. 23).

The diameter of the ordered domains depends upon the cooling rate and the alloy composition and may vary over several orders of magnitude.

Fig. 24 shows an example of very fine APBs in an  $\text{Ni}_3\text{Fe}$  alloy.

### 6.4.2.3 APBs produced by deformation, superlattice dislocations

On account of the differently occupied lattice sites, slip in an ordered phase through a Burgers vector  $b$ , which would cause no change of the lattice periodicity in a disordered crystal with the same basic structure, produces an APB along the slip plane (Fig. 20). This defect is removed by the passage of a second dislocation in the same slip plane. For the B2 and  $\text{DO}_3$  structures treated here, the possible arrangements of dislocations which would leave behind an undisturbed crystal are shown in Fig. 25. Such combinations are known as superlattice dislocations. Between the individual dislocations is an APB, which is responsible for the coupling of the dislocations to one another.

A superlattice dislocation is made up of two ordinary dislocations in the B2 structure and four dislocations in  $\text{DO}_3$  ordered crystals. The strain fields of the individual dislocations cause repulsive forces, and the APB between the dislocations results in an attractive force. These forces are equal in equilibrium. An example is shown in Fig. 26, where the contrast conditions have been chosen to reveal the dislocations clearly. In Fig. 27 the same area is imaged with a superlattice spot, so the APB contrast between the dislocations is revealed. The specimen was prepared in such a way that the operating slip plane was parallel to the foil surface.

Normally, a slightly deformed ordered solid solution will show a dislocation structure as in Fig. 28. The iron alloy with 12 at. % Si is B2 ordered. The dislocations are practically all doubled.

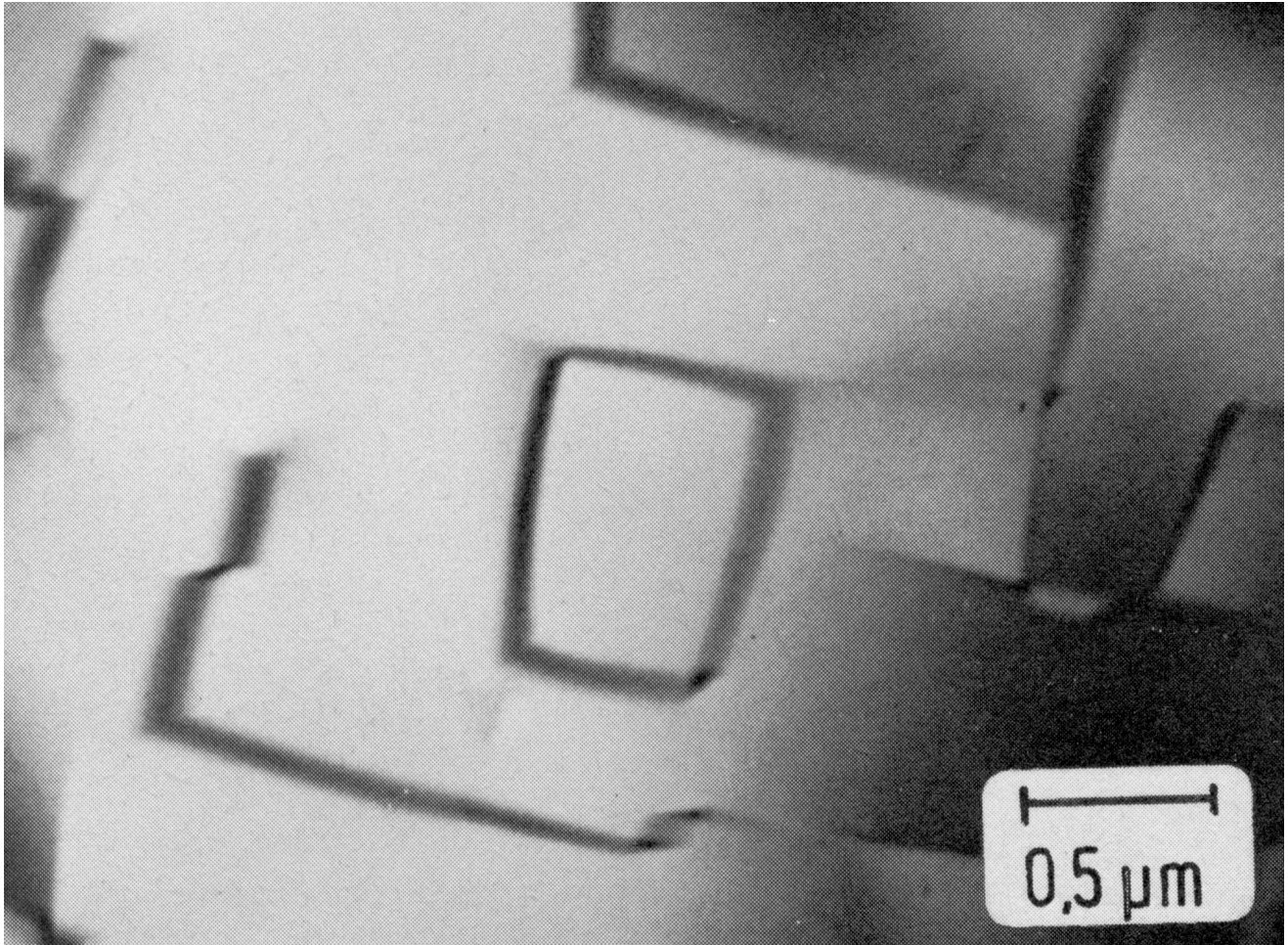


Fig. 22: Contrast reversal on an antiphase boundary, iron alloy with 14.1 % Si  
1000 °C 4 h + 627 °C 14 d/water, dark field image with  $\text{DO}_3$ -superlattice spot, thin foil

Bragg orientation



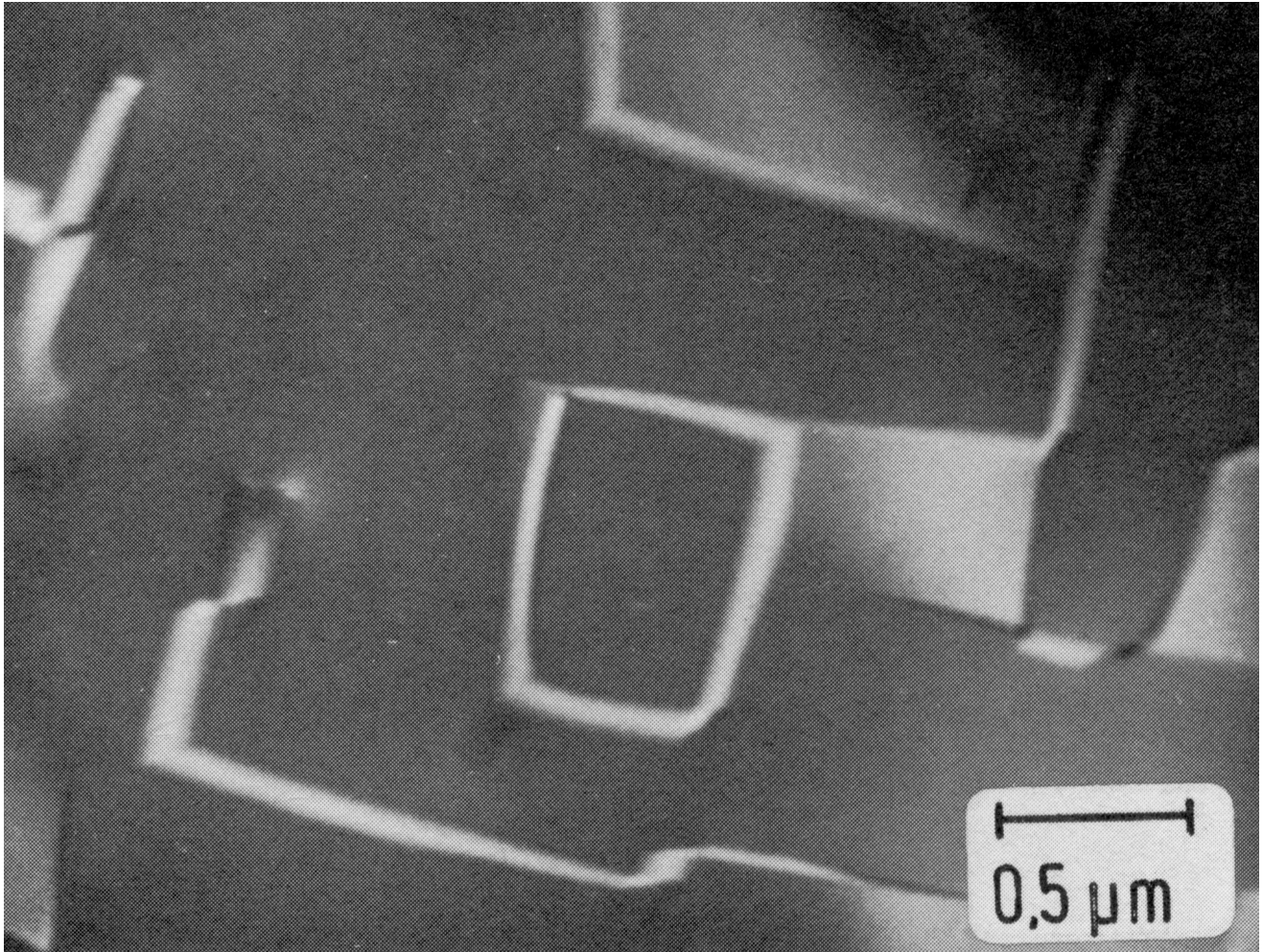


Fig. 23: Contrast reversal on an antiphase boundary, iron alloy with 14.1 % Si  
1000 °C 4 h + 627 °C 14 d/water, dark field image with DO<sub>3</sub>-superlattice spot, thin foil

slightly tilted with respect to [Fig. 22](#).



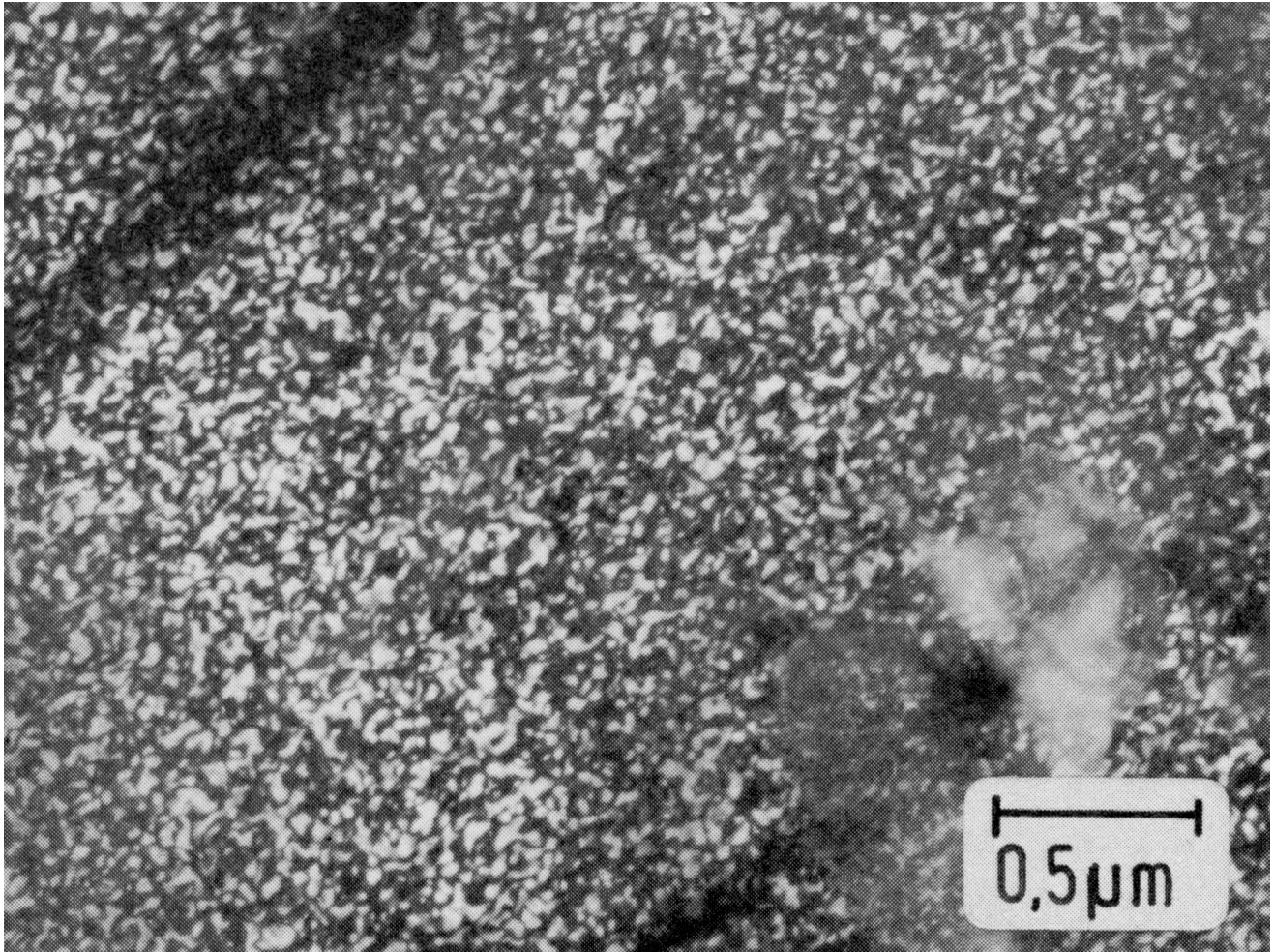


Fig. 24: Very fine antiphase boundaries, Ni<sub>3</sub>Fe-alloy  
1002 °C 5 d/air + 501 °C 56 d/water  
dark field image L<sub>1</sub><sub>2</sub>-superlattice spot, thin foil

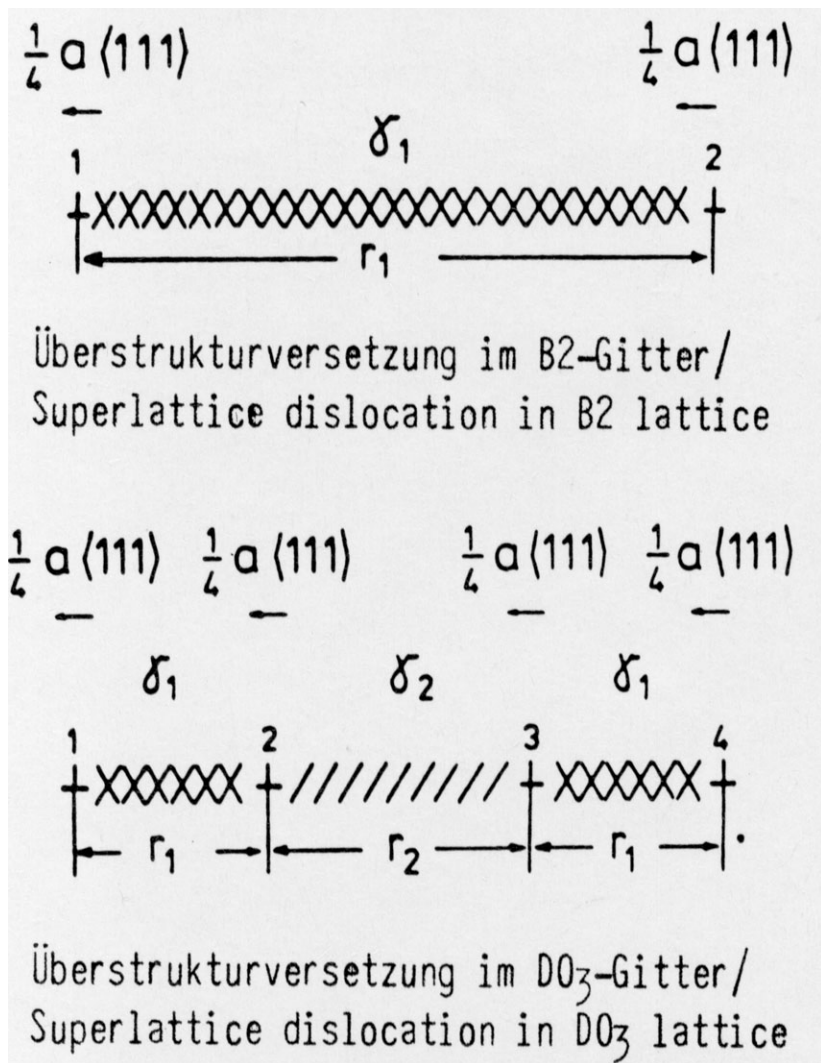


Fig. 25: Dislocation in ordered crystals with B2 and DO<sub>3</sub> structure. The indexing refers to the unit cell of the DO<sub>3</sub> lattice

$\gamma_1$ : antiphase boundary with disturbed nearest neighbours

$\gamma_2$ : antiphase boundary with disturbed next nearest neighbours



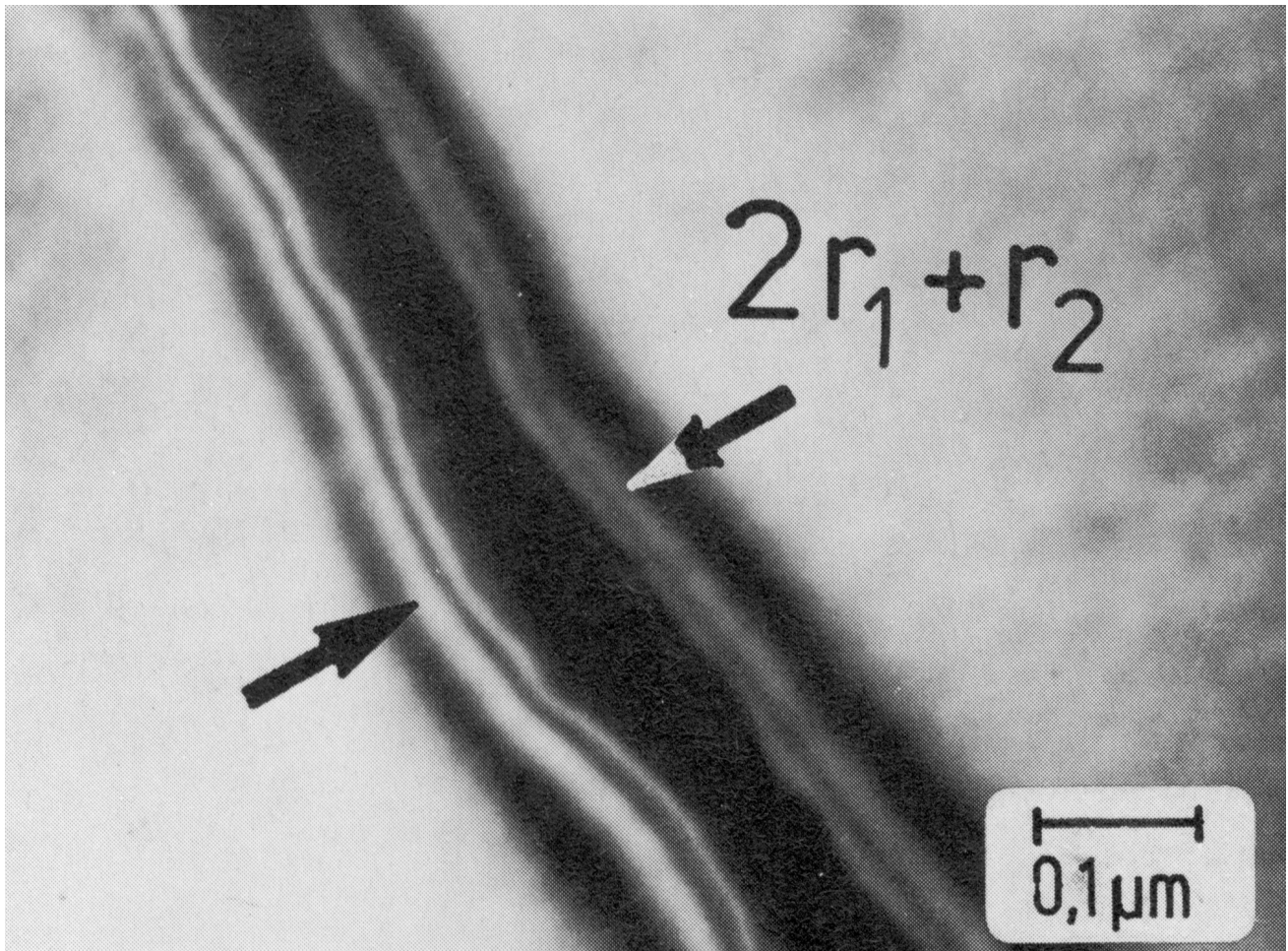


Fig. 26: Superlattice dislocation in DO<sub>3</sub> lattice, iron alloy with 14.85 Si, thin foil

dark field image with matrix spot



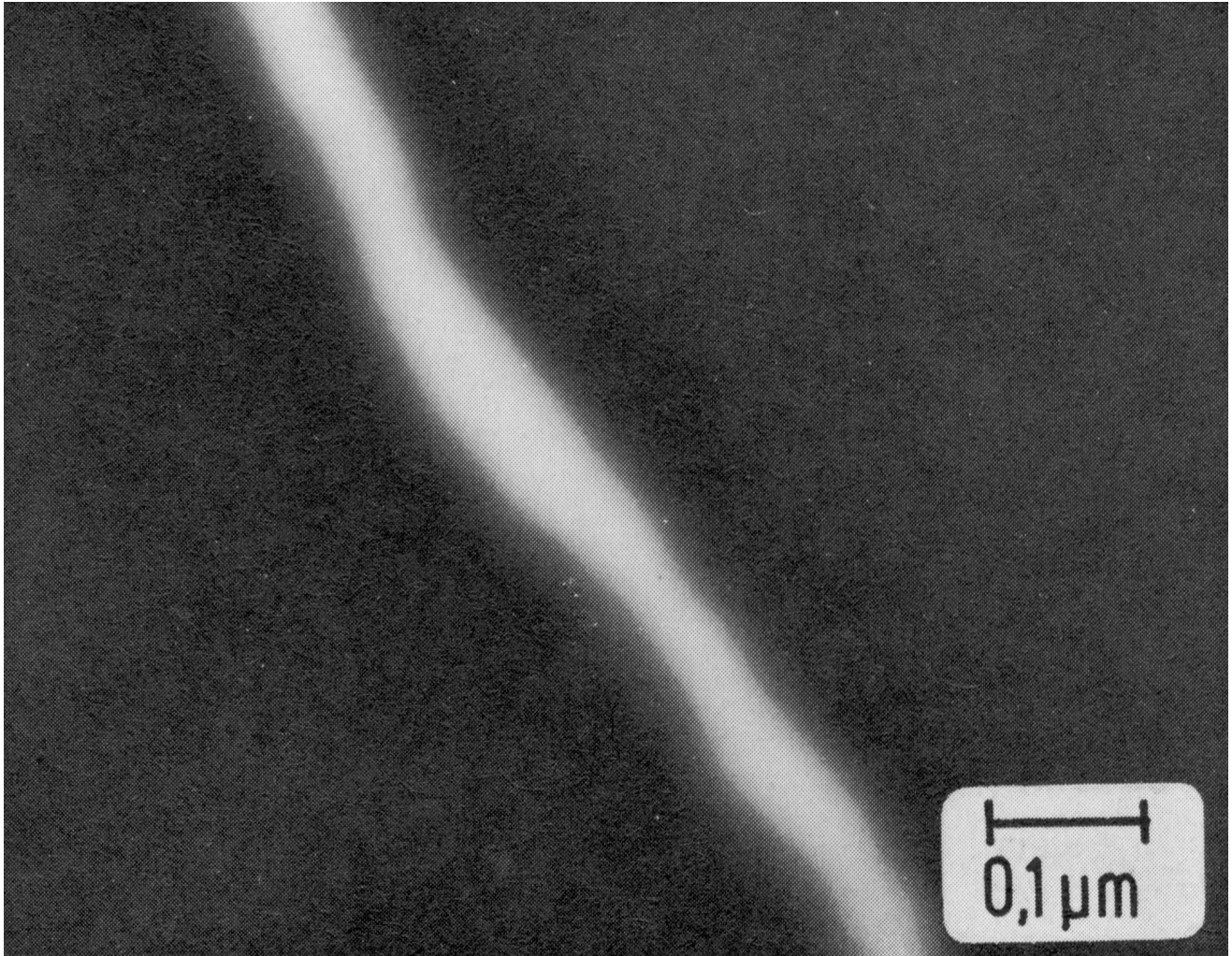


Fig. 27: Superlattice dislocation in DO<sub>3</sub> lattice, iron alloy with 14.85 % Si, thin foil

dark field image with DO<sub>3</sub> spot



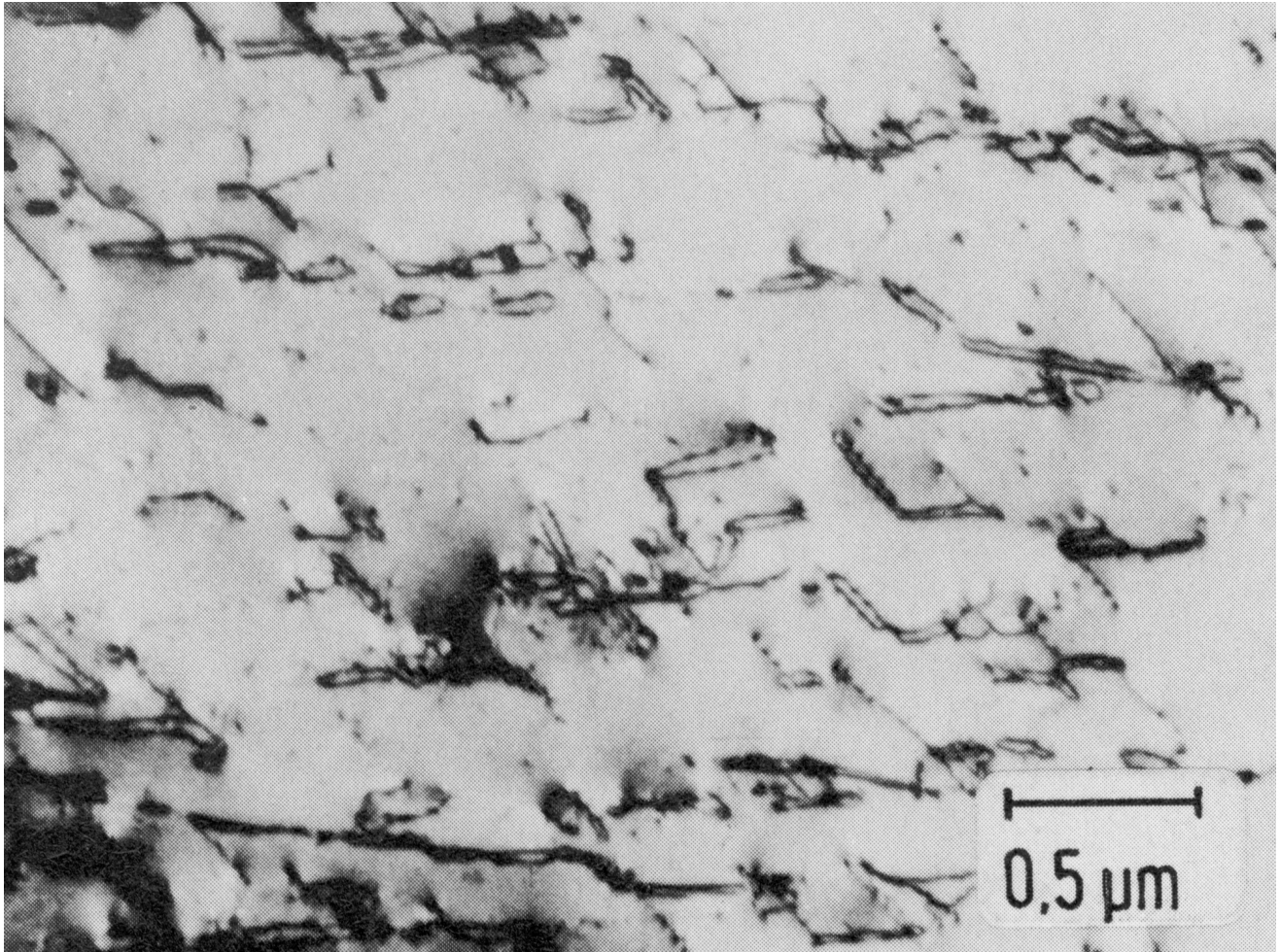


Fig. 28: Double dislocation in a B2-ordered alloy (iron with 12 % Si),  
bright field image, thin foil

In many cases, however, no complete superlattice dislocations move through the crystal. Slip planes on which no complete superlattice dislocations, but only single dislocations have moved are marked by APBs and may be imaged by superlattice spots. APBs formed by deformation lie on particular lattice planes (Fig. 29). The difference in the dislocation structure in comparison with disordered crystals is certainly one reason for the change in mechanical properties caused by ordering.

#### 6.4.2.4 Coherent, ordered precipitates

Ordering may take place as a first order phase transformation, i.e. with concentration splitting in a two-phase region, or as a homogeneous transformation of higher order. The formation of a two-phase region in first order transformations may take place, depending upon the temperature and the alloy composition, as a spinodal decomposition. However, nucleation on lattice defects has also been observed.

In an ordering transformation there is no change in the geometrical arrangement of the lattice sites, but simply a change in the occupation, so that the ordered precipitates are usually coherent. Since the lattice parameters of the ordered phase generally differ from these of the disordered matrix, coherency strains occur around the precipitates. If these strains are small, they will not affect the shape of the particles. At larger deviations of the lattice parameters, as in the case of the iron-silicon system, lattice distortions and plate-shaped coherent precipitates result.

The typical appearance of a two-phase microstructure with coherent, ordered precipitates nucleated by spinodal decomposition is shown in Fig. 30 and Fig. 31. The best contrast is obtained with a superlattice spot of the precipitate. As a consequence of the cubic symmetry and the coherence with the matrix, all precipitates appear bright simultaneously in the dark field micrograph, Fig. 30. The material is an iron alloy with 12 at. % Si which was annealed at 561 °C in the B2+DO<sub>3</sub> two-phase region. The DO<sub>3</sub> phase has precipitated in the form of plates on the {100} planes of the matrix. Fig. 31 shows the same area imaged with a B2 spot. The foil shows a continuous zone of high diffraction



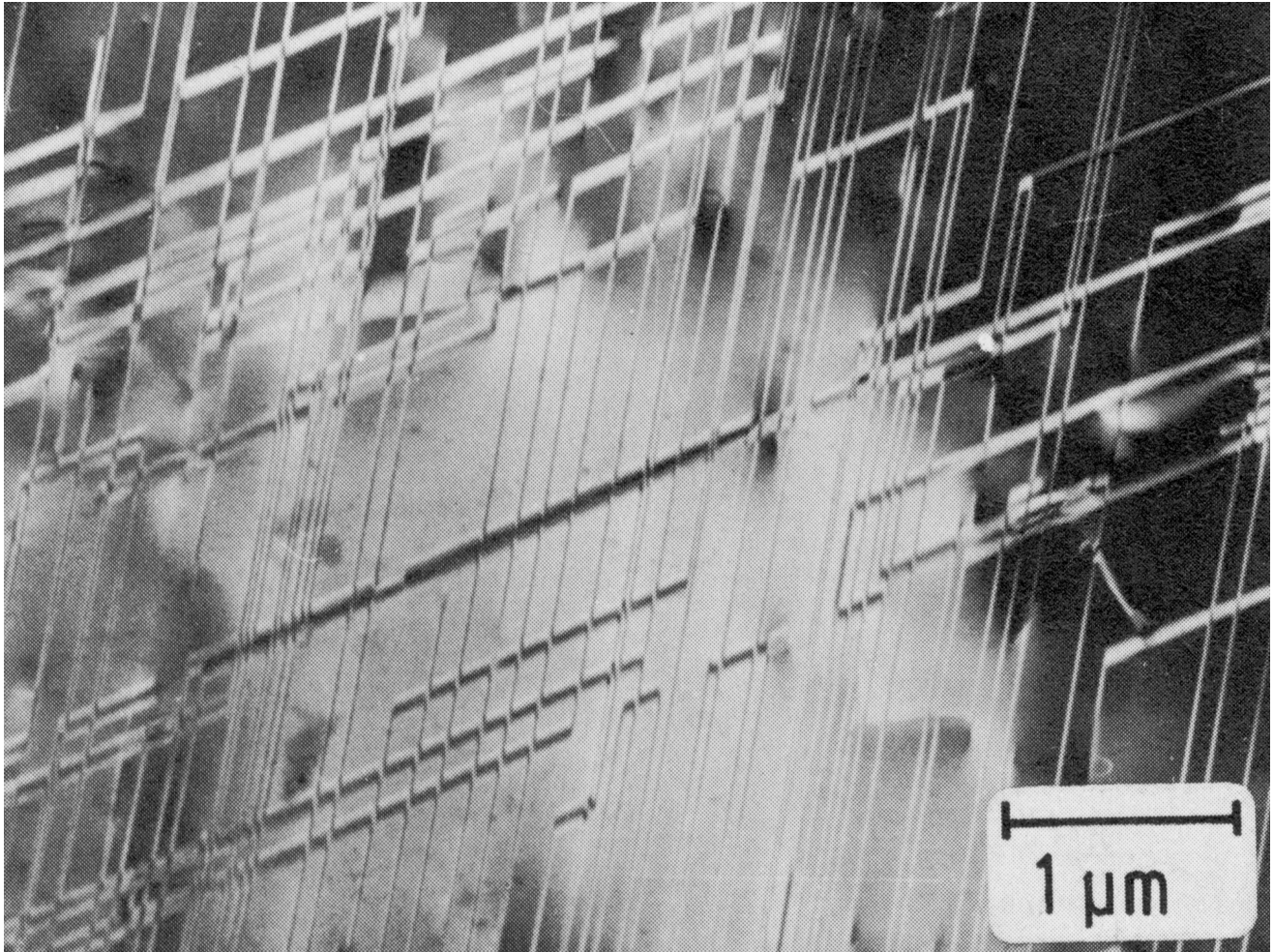


Fig. 29: Antiphase boundaries on glide planes produced by deformation, Fe<sub>3</sub>Si alloy, 0.5 %deformed, dark field image with DO<sub>3</sub>-superlattice spot, thin foil



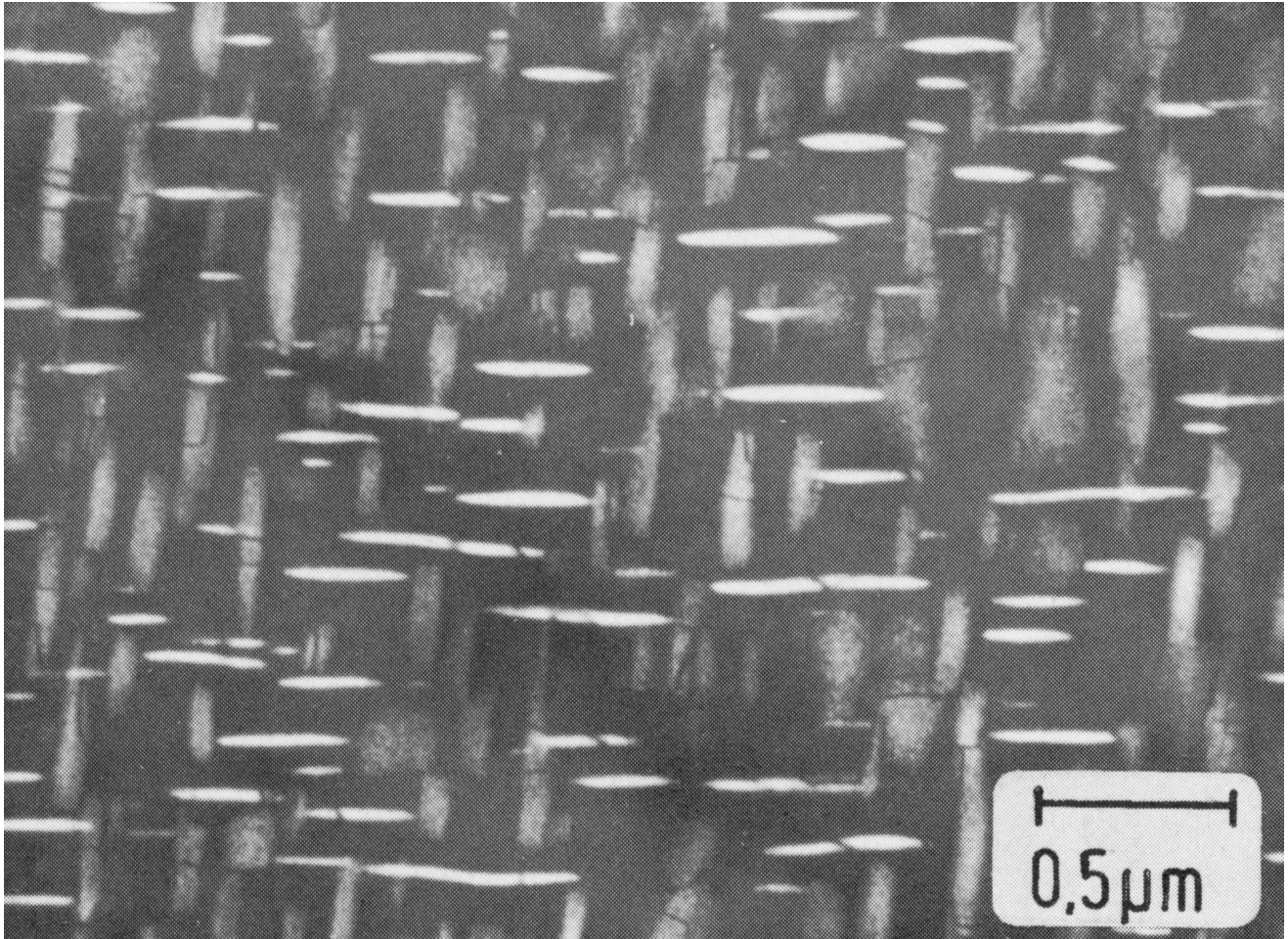


Fig. 30: Coherent DO<sub>3</sub> precipitates in a B2 matrix, iron alloy with 11.3 % Si, 561 °C 14 d/water, thin foil

dark field image with DO<sub>3</sub>-superlattice spot



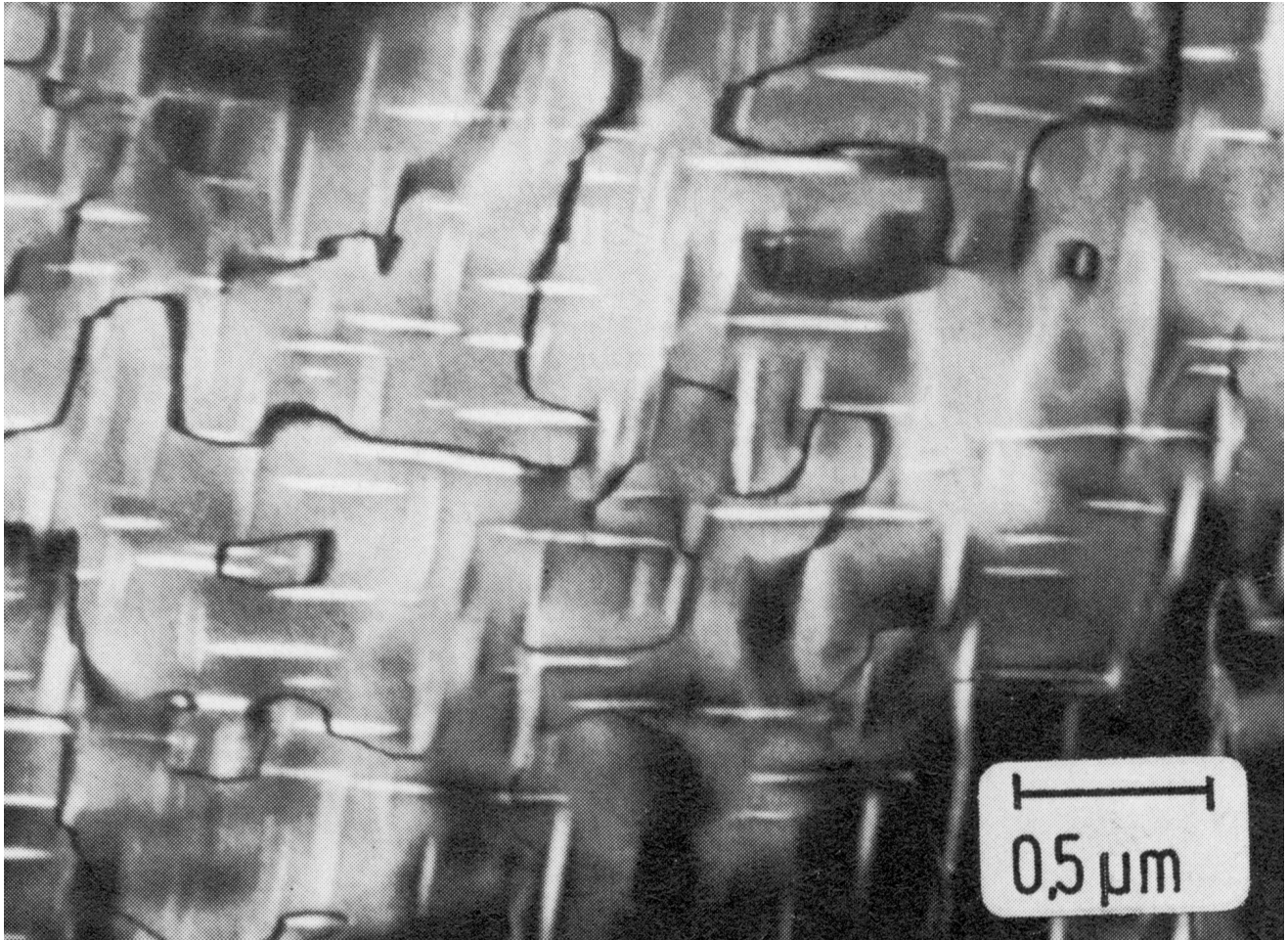


Fig. 31: Coherent DO<sub>3</sub> precipitates in a B2 matrix, iron alloy with 11.3 % Si, 561 °C 14 d/water, thin foil

dark field image with B2-superlattice spot



intensity with increased brightness in the  $\text{DO}_3$  precipitates and curved, thermal B2 APBs. In an image using a matrix spot only the strain contrast may be seen.

Due to the different chemical properties of the phases, differences in thickness may arise during preparation of the thin foil. If the coarsening of the precipitates is sufficiently advanced, they can be seen in the bright field image on account of the difference in thickness (Fig. 32, iron alloy with 15.3 at. % Si, aged at 675 °C in the B2+ $\text{DO}_3$  range).

### Literature

- 6) Marcinkowski, M.J. in: Electron Microscopy and Strength of Crystals, John Wiley and Sons, New York 1963.
- 7) Schlatte, G.: Dissertation, RWTH Aachen 1975.

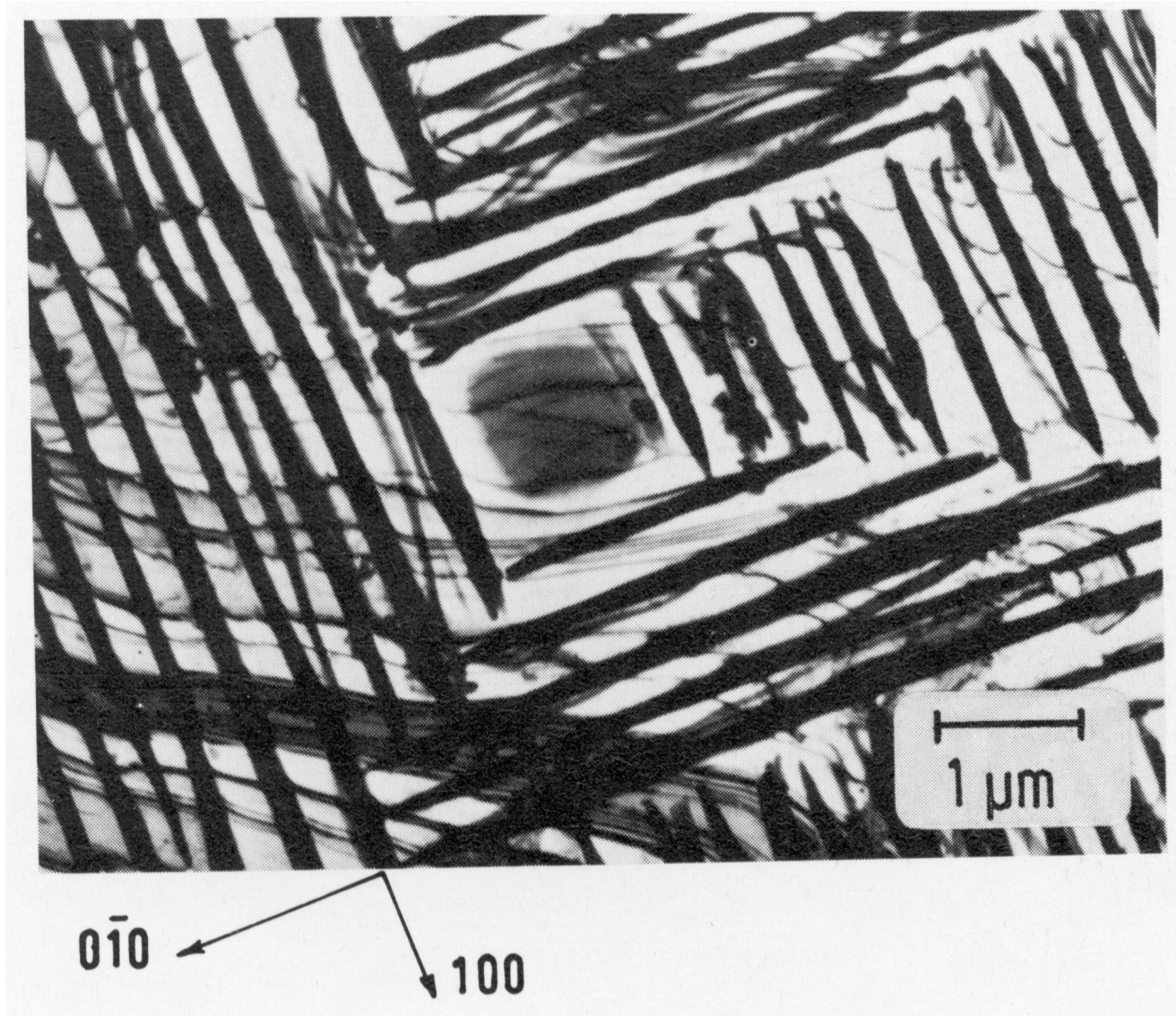


Fig. 32: B2 + DO<sub>3</sub> two-phase structure iron alloy with 13.3 % Si, 675 °C 14 d/water  
bright field, thin foil